Ab-initio Calculations to Model Anomalous Fluorine Behavior

Milan Diebel[1] and Scott T. Dunham[2]

[1]Department of Physics, University of Washington, Seattle, WA 98195-1560, USA

[2]Department of Electrical Engineering, University of Washington, Seattle, WA 98195-2500, USA

ABSTRACT

Implanted fluorine has been observed to behave unusually in silicon, manifesting apparent uphill diffusion [1]. We are further motivated to understand the behavior of implanted fluorine in silicon by experiments which suggest that fluorine reduces boron diffusion [2, 3, 4, 5] and enhances boron activation in shallow junctions [2, 3]. In order to investigate fluorine behavior, we calculated the energy of fluorine defect structures in the framework of density functional theory (DFT). Besides identifying the ground-state configuration of a single fluorine atom in silicon, a set of energetically favorable fluorine defect structures were found. The latter strongly suggests a distinct fluorine diffusion mechanism, which was implemented in a continuum diffusion simulation and compared to experimental data.

INTRODUCTION

As ULSI devices enter the nanoscale, ultra-shallow junctions become necessary. Reduction in transient enhanced diffusion (TED) and enhanced dopant activation are desired. Experimentally, fluorine has shown to have beneficial properties on both boron TED reduction [2, 3, 4, 5] as well as boron activation [2, 3]. However, to utilize these benefits effectively, a fundamental understanding of F behavior is necessary, particularly since F shows anomalous diffusion behavior [1]. Figure 3 shows data reported by Jeng *et al.* In the experiment, 10^{13}cm^{-2} F$^+$ was implanted at 30 keV and annealed for 30 min at various temperatures.

The anomaly consists of two key features. At temperatures below 550°C, no noticeable F diffusion takes place. However, at higher temperatures, rapid F diffusion is reported. Such a behavior indicates the formation of strongly bound F complexes, since ab-initio calculations give a migration barrier of only 0.7-1.3 eV, which indicates that interstitial F (F_i) is a highly mobile species [8, 9]. The second part of the anomalous behavior is the shapes of the annealed profiles. Instead of a broadening, the annealed profiles sharpen and shift toward the surface.

RESULTS

The analysis is split into two sections. First, the ab-initio results are discussed. Then, a continuum model is developed using the first-principle data to compare to the anomalous fluorine behavior reported experimentally.

Ab-initio Calculations

In order to investigate fluorine behavior in silicon, the energies for various configurations were calculated using the DFT code VASP [10] with a PW91 GGA functional and ultra-soft

Structure	E_b last F [eV]	E_b^{tot} [eV]	E_f [eV]
FV	-2.38	-2.38	$+1.00$
F_2V	-2.25	-4.63	-1.25
F_3V	-1.95	-6.58	-3.20
F_4V	-0.54	-7.12	-3.74
V_2	—	-1.45	$+5.31$
FV_2	-2.75	-4.20	$+2.56$
F_2V_2	-2.87	-7.07	-0.31
F_3V_2	-1.97	-9.04	-2.28
F_4V_2	-2.43	-11.47	-4.71
F_5V_2	-1.82	-13.29	-6.53
F_6V_2	-1.80	-15.09	-8.33

Table 1: Binding energies of F_nV_m configurations. The decreasing binding energy of the F_nV structures is attributed to the increasing crowding of the F atoms. This phenomenon is illustrated in Fig. 1. The total binding energies (third column) are calculated with respect to interstitial fluorine (F_i) and single vacancies (V). The binding energies in the second column are the energy change in adding an additional F to the structure. The fourth column lists the total formation energy, which includes the formation energy of the necessary vacancies.

Vanderbilt-type pseudo-potentials [11]. All calculations were performed in a 64 atom super-cell with periodic boundary conditions and $2 \times 2 \times 2$ Monkhorst-Pack **k**-point sampling with an energy cut-off of 320 eV. The structures were fully relaxed requiring a maximal force of 0.005 eV/Å per atom. In addition to fluorine structures, interstitial (I), and vacancy (V) ground-state energies were calculated as references. The calculated formation energies of I and V are 3.78 eV and 3.38 eV respectively.

In its ground-state, a single F atom prefers to reside in a bond center interstitial site. This site is preferred by 0.18 eV over the tetrahedral interstitial configuration and by 1.00 eV over the lowest substitutional site. The same reference structure was found by Taguchi et al. [9]. DFT calculations show interstitial F to be highly mobile ($E_{F_i^{bc}}^m \leq 1.3$ eV [9], $E_{F_i^{tet}}^m = 0.7$ eV [8]). However, we found F_nV_m structures to have a rather high binding energy, suggesting decoration of vacancies by fluorine. In Table 1, the formation and binding energies for different F_nV_m configurations are listed. Here the reference point for the total binding energy is interstitial fluorine and single vacancies.

For two or more F atoms, F_nV_m structures are favored over the interstitial configuration. For F_nV structures, the binding energy gained by adding an additional fluorine atom decreases. This behavior is due to the increasing space requirement of the decorating fluorine atoms. This becomes particularly apparent by comparing F_2V with F_3V in Fig. 1. Three fluorine atoms in F_3V are pushed away from each other and a distortion of the surrounding silicon lattice is noticeable. The rather large drop in marginal binding energy between F_3V and F_4V from 1.95 eV to 0.54 eV can be explained with the same argument, since F_4V shows an increasing distortion of the lattice and the bond length (see Fig. 1).

We also investigated F_nV_2 structures, which also show a reduction in binding energy with n, but no sharp drop-off, since more space is available to accommodate all F atoms.
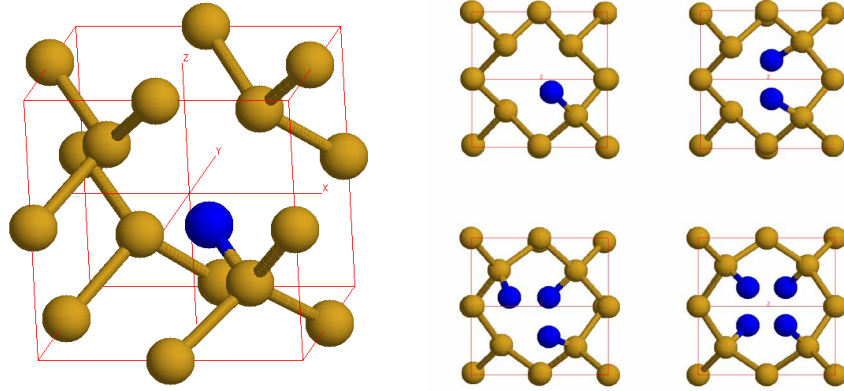
C4.5.2

Figure 1: Left: 3D view of a single FV complex. The fluorine atom has moved toward the silicon out of the substitutional silicon site. The Si–F bond length is 1.68 Å (71% of the Si–Si bond length). The silicon atoms are drawn in amber (light), while the fluorine atom is presented in blue (dark). Right: View down the $\langle 100 \rangle$ direction (see Fig. 2 left) of the four F_nV structures. An increasing distortion of the surrounding silicon lattice is observed when adding more fluorine atoms. This is due to the repulsion of the F atoms, which becomes particularly apparent by comparing F_2V with F_4V.

The results are also listed in Table 1. In Fig. 2, the equilibrium concentrations at 600°C and 1000°C of F structures versus total F concentration are shown. In the presence of non-equilibrium point defect concentrations, the local equilibrium F_nV_m concentrations need to be multiplied by $(C_V/C_V^*)^m$. Thus, in the presence of excess vacancies during initial stages of implant anneals, almost all fluorine will reside in F_nV_m structures. The evolution of F_nV_m clusters is particularly important during implant anneals due to the high point defect concentrations.

The saturated F_6V_2 structure shows another interesting property: it is stable in the presence of interstitials. Table 2 lists the energy change associated with I reactions with F_nV_m structures. Migration barriers, which might further stabilize F_nV_m structures, are not included. Due to the entanglement of the fluorine atoms with the surrounding silicon lattice, we believe these defects to be immobile.

We also investigated pairing of F_i with I and F_i. DFT predicts interstitial F_2 to be unbound, as the fluorine prefers to remain in an interstitial site rather than forming an F_2 bound-state. F_i binds to I with an energy of 0.46 eV. This number was deduced by comparing FI to F_i and I separated within the same super-cell. This energy difference agrees well with a pure Coulombic model of FI binding as F^-I^+ (separating e^+ and e^- in a silicon environment an equivalent distance leads to an energy difference of 0.50 eV).

Continuum Model

To model fluorine diffusion in the continuum limit, we implemented fluorine decoration of V and V_2. All energetically favorable reactions are treated as diffusion limited and we
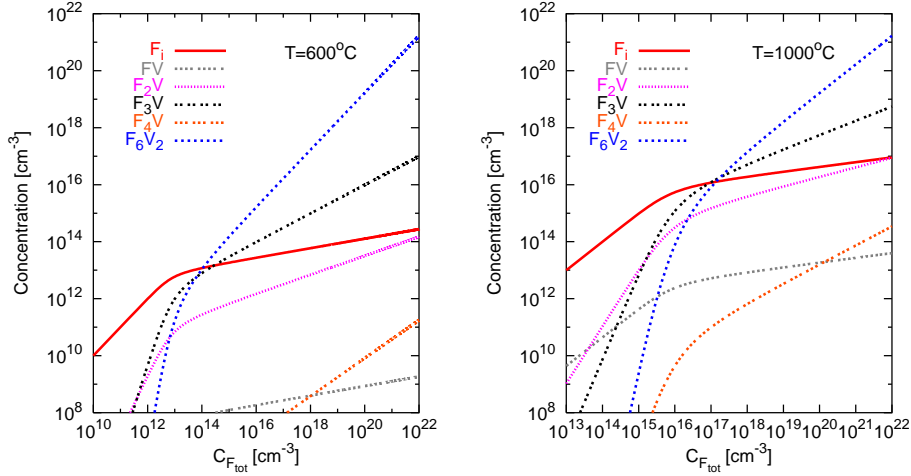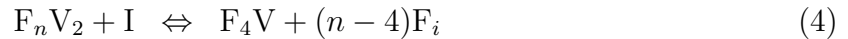
Figure 2: Equilibrium concentration of various F_nV_m structures vs. total F concentration at 600°C and 1000°C. Qualitatively the behavior for both temperatures is similar. For low $C_{F_{tot}}$ the dominant species is F_i due to the entropy of mixing. At high $C_{F_{tot}}$ the major F contribution comes from F_6V_2 clusters. The vacancy formation energy is included in these calculations.

considered only I, V, and F_i to be mobile in the Si phase. The associated formation and dissociation reactions are:

$$F_nV_m + F_i \Leftrightarrow F_{n+1}V_m \tag{1}$$

$$F_i + I \Leftrightarrow FI \tag{2}$$

$$F_nV + I \Leftrightarrow nF_i \tag{3}$$

$$F_nV_2 + I \Leftrightarrow F_4V + (n-4)F_i \tag{4}$$

$$FI + V \Leftrightarrow F_i \tag{5}$$

In addition, extended defect models, including I_n and V_n clusters up to size $n = 10$ plus {311} defects, are used [6]. The extended defect models are crucial for the correct temperature behavior. To match the experimental set up, a thin oxide surface layer of 20 Å is included in the simulation. To limit the number of free parameters, the oxide layer is treated in a very simple way. Only segregation at the interfaces and diffusion of F_i are considered in this phase.

Figure 3 shows the simulation results compared to the experimental data. Qualitatively the correct F behavior is observed, however the simulations show a somewhat stronger temperature dependence than observed experimentally. At 550°C, no significant movement is predicted, while at 850°C, F is entirely removed from silicon. A possible reason for the shortcomings at 550°C might be the fact that the model does not include mobile I_2, which are predicted by ab-initio calculations [7]. We expect I_2 to change the profiles especially in the I-rich tail regions, where mobile I_2 will annihilate V_n clusters, reducing F decoration. The discrepancy at higher T may be due to the fact that we only include V and V_2 decoration. The ab-initio calculations suggest that a complete model need to include also the decoration of larger V_n clusters, since large binding energies are anticipated. Larger more stable F_nV_m clusters can be expected to remain in the V-rich region near the surface. The F signal near the surface might be also due to knock-ons from F segregation to the Si/SiO$_2$ interface on

C4.5.4

$F_n V + I \Leftrightarrow n F_i$	ΔE [eV]
$n = 1$	+4.78
$n = 2$	+2.53
$n = 3$	+0.58
$n = 4$	+0.04
$F_n V_2 + I \Leftrightarrow F_4 V + (n-4) F_i$	ΔE [eV]
$n = 4$	+2.81
$n = 5$	+0.99
$n = 6$	−0.81

Table 2: Stability of the $F_n V_m$ cluster in the presence of I. ΔE is defined as $E_{F_n V_m + I} - E_{rhs}$. Our calculations find that the fully saturated $F_6 V_2$ structure is stable even at high I concentrations. This calculation does not include possible migration barriers, which further stabilize $F_n V_m$ structures.

oxide film.

CONCLUSIONS

Ab-initio calculations predict strongly bound $F_n V_m$ clusters. No other comparably stable structures were identified; the binding energy found for FI clusters is significantly smaller. This DFT data was used to identify the diffusion mechanism which was implemented in a continuum model to explain the anomalous fluorine behavior reported by Jeng et al. Fast diffusing F_i decorate V_n forming immobile $F_n V_m$ clusters. At higher temperatures, these clusters get annihilated by I. Thus, F decoration of V leads to F dissolving from deeper regions (I excess) and accumulation near surface (V excess). Due to the strong affinity of F for V, for pre-amorphized samples we expect incorporation of $F_n V_m$ clusters during regrowth. The consequences for boron diffusion in such an environment would be TED reduction and activation for amorphizing conditions due to excess V. However, in the case of non-amorphizing implants we expect an increased I concentration due to the formation of $F_n V_m$ clusters, which leads to an enhancement of TED. The predictions for amorphizing conditions are supported by experimental data [2, 4, 5].

ACKNOWLEDGMENTS

REFERENCES

[1] S.-P. Jeng, T.-P. Ma, R. Canteri, M. Anderle, and G.W. Rubloff, Appl. Phys. Lett. **61**, 1310 (1992).
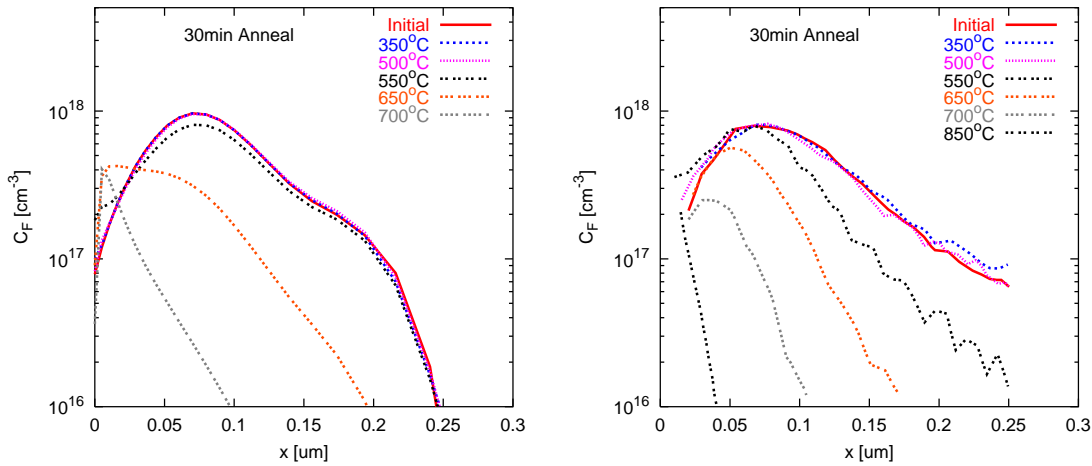
Figure 3: Comparison of simulation (left) with experimental data [1] (right) for 10^{13}cm^{-2} 30 keV F$^+$ implant annealed for 30 min at various temperatures. The simulation includes F$_n$V, F$_n$V$_2$, and FI clusters in addition to an extended defect model [6]. The initial defect/fluorine profiles were obtained with Monte Carlo implant simulator UT-Marlowe 6.0 and kinetic damage accumulation model.

[2] T.H. Huang and D.L. Kwong, Appl. Phys. Lett. **65**, 1829 (1994).

[3] J. Park and H. Hwang in *Si Front-End Processing: Physics and Technology of Dopant-Defect Interactions*, edited by H.-J. L. Gossmann, T.E. Haynes, M.E. Law, A.N. Larsen, and S. Odanaka, (Mater. Res. Soc. Symp. Proc. **568**, Warrendale, PA, 1999) pp. 71-75.

[4] D.F. Downey, J.W. Chow, E. Ishida, and K.S. Jones, Appl. Phys. Lett. **73**, 1263 (1998).

[5] L.S. Robertson, P.N. Warnes, K.S. Jones, S.K. Earles, M.E. Law, D.F. Downey, S. Falk, and J. Liu in *Si Front-End Processing: Physics and Technology of Dopant-Defect Interactions II*, edited by A. Agarwal, L. Pelaz, H-H. Vuong, P. Packan, M. Kase, (Mater. Res. Soc. Symp. Proc. **610**, Warrendale, PA, 2000) pp. B4.2.1-B4.2.6.

[6] P. Fastenko, S.T. Dunham, and S. Chakravarthi presented at the 2002 MRS Spring Meeting, San Francisco, CA, 2002 (published in this proceeding).

[7] S. K. Estreicher, M. Gharaibeh, P.A. Fedders, and P. Ordejón, Phys. Rev. Lett. **86**, 1247 (2001).

[8] C.G. Van de Walle, F.R. McFeely, and S.T. Pantelides, Phys. Rev. Lett. **61**, 1867 (1988)

[9] A. Taguchi and Y. Hirayama, Solid State Commun. **116**, 595 (2000).

[10] G. Kresse and J. Hafner, Phys. Rev. B **47**, RC558 (1993); G. Kresse and J. Furthmüller, **54**, 11169 (1996).

[11] D. Vanderbilt, Phys. Rev. B **41** 7892 (1990); G. Kresse and J. Hafner, J. Phys. Condens. Matter **6**, 8245 (1994).